



Estimating lockdown induced European NO₂ changes

5 Jérôme Barré¹, Hervé Petetin², Augustin Colette³, Marc Guevara², Vincent-Henri Peuch¹, Laurence Rouil³, Richard Engelen¹,
Antje Inness¹, Johannes Flemming¹, Carlos Pérez García-Pando^{2,4}, Dene Bowaldo², Frederik Meleux³, Camilla Geels⁵,
Jesper H. Christensen⁵, Michael Gauss⁶, Anna Benedictow⁶, Svetlana Tsyro⁶, Elmar Friese⁷, Joanna Struzewska⁸, Jacek W.
Kaminski^{8,9}, John Douros¹⁰, Renske Timmermans¹¹, Lennart Robertson¹², Mario Adani¹³, Oriol Jorba², Mathieu Joly¹⁴,
Rostislav Kouznetsov¹⁵

10 ¹ European Centre for Medium-range Weather Forecast (ECMWF), Sinfield Park, Reading, UK

² Barcelona Supercomputer Centre (BSC), Barcelona, Spain

³ National Institute for Industrial Environment and Risks (INERIS), Verneuil-en-Halatte, France

⁴ ICREA, Catalan Institution for Research and Advanced Studies, Barcelona, Spain

⁵ Department of Environmental Science, Aarhus University, Roskilde, Denmark

15 ⁶ Norwegian Meteorological Institute, Oslo, Norway

⁷ Rhenish Institute for Environmental Research at the University of Cologne, Cologne, Germany

⁸ Institute of Environmental Protection - National Research Institute, Warsaw, Poland

⁹ Faculty of Environmental Engineering, Warsaw University of Technology, Warsaw, Poland

¹⁰ Royal Netherlands Meteorological Institute (KNMI), De Bilt, the Netherlands

20 ¹¹ Netherlands Organisation for Applied Scientific Research (TNO), Climate Air and Sustainability Unit, Utrecht, the
Netherlands

¹² Swedish Meteorological and Hydrological Institute (SMHI), Norrköping, Sweden

¹³ Italian National Agency for New Technologies, Energy and Sustainable Economic Development (ENEA), Bologna, Italy

¹⁴ Météo-France, Toulouse, France

25 ¹⁵ Finnish Meteorological Institute (FMI), Helsinki, Finland

Correspondence to: Jérôme Barré (jerome.barre@ecmwf.int)

Abstract. This study provides a comprehensive assessment of NO₂ changes across the main European urban areas induced by
the COVID-19 lockdown using satellite retrievals from the Tropospheric Monitoring Instrument (TROPOMI), surface site
30 measurements and simulations from the Copernicus Atmospheric Monitoring Service (CAMS) regional ensemble of air quality
models. Some recent TROPOMI-based estimates of NO₂ changes have neglected the influence of weather variability between
the reference and lockdown periods. Here we provide weather-normalized estimates based on a machine learning method



(gradient boosting) along with an assessment of the biases that can be expected from methods that omit the influence of weather. We also compare the weather-normalized satellite NO₂ column changes with both weather-normalized surface NO₂ concentration changes and simulated changes by the CAMS regional ensemble, composed of 11 models, using recently published emission reductions induced by the lockdown. We show that all estimates show the same tendency on NO₂ reductions. Locations where the lockdown was stricter show stronger reductions and, conversely, locations where softer measures were implemented show milder reductions in NO₂ pollution levels. Regarding average reductions, estimates based on either satellite observations (-23%) surface stations (-43%) or models (-32%) are presented, showing the importance of vertical sampling but also the horizontal representativeness. Surface station estimates are significantly changed when sampled to the TROPOMI overpasses (-37%) pointing out the importance of the variability in time of such estimates. Observation based machine learning estimates show a stronger temporal variability than the model-based estimates.

1. Introduction

Nitrogen dioxide (NO₂) is part of the nitrogen oxides (NO_x=NO+NO₂) and a very well-established cause of poor air quality in the most urbanized and industrialized areas of the world. NO₂ is harmful for living organisms over long term atmospheric concentration exposure. It also plays a major role in urban ozone formation and secondary aerosols which are also harmful for the living at high levels in the lower atmosphere (Lelieveld et al., 2015; Myhre et al., 2013). According to the European Environment Agency (EEA 2020a) European main anthropogenic NO_x sources are road transport (39%), energy production and distribution (16%), commercial, residential and households (14%), energy use in industry (12%), agriculture (8%), non-road transport (8%) and industrial processes and product use (3%). With an atmospheric lifetime typically below 1 day, NO_x is relatively short-lived and is mainly controlled by photochemical reactions, so the majority of NO_x does not get transported far downwind from its sources (Seinfeld and Pandis, 2006). Thus, near-surface NO_x concentration is high over cities and densely populated areas and low otherwise. Besides emissions, the variability of NO_x is strongly driven by meteorological conditions, especially atmospheric transport, vertical mixing and solar radiation that can favour or not their accumulation close to emission sources (Arya, 1999). Its short lifetime combined with localized emission sources make NO₂ an excellent proxy for detecting emission reductions, from both surface and satellite measurements.

The worldwide outbreak of the coronavirus disease (COVID-19) that arose in late 2019 in China and spread around the world in early 2020 led many countries to take action in order to slow down the contamination growth rate of the virus. The so-called lockdowns severely restricted or banned movements of people, closed most public places and limited journeys to essential work commutes. Some measures started in China in late 2019 with stricter lockdowns in January 2020. In Europe, lockdown measures were implemented at various dates during February and March 2020. These lockdowns drastically reduced traffic and also activity levels in most industries (Guevara et al., 2020; Le Quéré et al., 2020). These sectors represent a large share of NO_x emissions (51% according to EEA 2020a).



65 The lockdowns are expected to have large effects on urban NO₂ air pollution levels. A number of studies used surface
measurement sites. For example, Wang et al. (2020a) showed that lower emissions from motor vehicles and secondary
industries were most likely responsible for the observed decreases of NO₂ concentrations in China during January-March 2020.
Collivignarelli et al. (2020) showed that major NO₂ reductions occurred in Milan, a city that showed rapid increase of cases
early in the European COVID-19 crisis (February 2020) and was one of the first cities to be put into lockdown in Europe.
70 Accounting for the effect of the meteorological variability, Petetin et al. (2020), highlighted a strong reduction of surface NO₂
concentrations across most Spanish urban areas during the first weeks of lockdown.

The first quarter of 2020 had specific and very changing meteorological conditions. The storm Ciara crossed over
Europe in the second week of February followed by the storm Dennis that also crossed Europe a week later. Both extratropical
storms generated strong winds over the northern half of Europe (above 45°N) from February 9th, 2020 until February 18th,
75 2020. Strong wind situations, yet milder, over the Iberian Peninsula, the southern part of France and the northern part of Italy
were also generated by storms Karine and Myriam in the first week of March. Moreover, February and March 2020 displayed
stronger positive temperatures anomalies over Europe in comparison with February and March 2019
(<https://surfobs.climate.copernicus.eu/stateoftheclimate>). Such weather anomalies however did not persist further during the
second quarter of 2020. Air quality modelling prediction systems represent the evolution of pollutants in the atmosphere
80 accounting for changes in weather using numerical weather prediction data. The Copernicus Atmospheric Monitoring Service
(CAMS) produces European air quality forecasts and analyses daily using an ensemble of 11 models and the European Centre
for Medium-range Weather Forecasts (ECMWF) data as input ensuring unique reliability and quality (Marecal et al., 2015).
Using scaling emission factors to account for lockdown measures such system can be used to estimate lockdown reductions
and account for the weather variability (Colette et al., 2020).

85 Several studies used the recently launched (October 2017) Tropospheric Monitoring Instrument (TROPOMI,
Veefkind et al., 2012) on board the Copernicus Sentinel-5 Precursor satellite to showcase the NO₂ reductions due to the
COVID-19 lockdown. Due to the young age of the instrument it is impossible to work with a climatological baseline that
would use at least several years to assess the lockdown reductions. Often satellite data from 2020 are compared with data from
2019 sometimes over short time periods. For example, Muhammad et al. (2020), compared full March 2019 averages with the
90 14-25 March 2020 average for Europe, amongst other estimates for other regions. Bauwens et al. (2020) provided a more in-
depth assessment of NO₂ column reduction estimates by using similar year to year methodology, i.e. comparing 2019 to 2020.
A number of TROPOMI NO₂ studies on COVID-19 lockdown reductions give little weight to the synoptic meteorological
conditions and how they could potentially flaw the estimates. Zambrano-Monserrate et al. (2020) and Nakada et al., (2020)
showed maps of TROPOMI for short time periods comparing 2020 with 2019 for Europe, Asia and South America with no
95 clear quantitative and robust assessment of the underlying weather conditions. Wang et al. (2020b), used differences of
TROPOMI NO₂ images over China before and during the lockdown to illustrate the impact of the lockdown on air pollution,
but do not emphasise on how those differences might be affected by differences in weather conditions. In contrast, Schiermeier
(2020) mentioned the ‘weather factor’ early on in the COVID-19 crisis which can affect strongly the pollution levels. And



100 studies as for example Le et al. (2020) showed 2019 and 2020 TROPOMI NO₂ comparisons but acknowledged the impact of
weather anomalies on pollution levels. Only very recently a weather-normalization technique has been applied to estimate NO₂
changes across cities in the US based on TROPOMI (Goldberg et al., 2020). Also, insufficient importance and clarity are given
about the fact that satellite data used in such analyses are conditioned by the cloud coverage, revisit frequency and quality flag.
Ignoring or not acknowledging such information can also lead to flawed satellite based estimates and provide misleading
information ([https://atmosphere.copernicus.eu/flawed-estimates-effects-lockdown-measures-air-quality-derived-satellite-
105 observations](https://atmosphere.copernicus.eu/flawed-estimates-effects-lockdown-measures-air-quality-derived-satellite-observations)).

In this paper, we aim to first illustrate how misleading it is to consider non-weather normalized TROPOMI estimates
for assessing changes in NO₂ induced by lockdown measures. We focus on Europe and provide a method that accounts for
weather variability or more broadly speaking estimates what TROPOMI would have measured in Spring 2020 under “business
as usual” (BAU) emission forcing (i.e. without any lockdown measures) in section 2. We then aim to provide a comprehensive
110 assessment of the European lockdown induced NO₂ changes. We compare the satellite estimates against what can be inferred
from surface observations that also account for weather variability in section 3. We compare also with model-based scenarios
using ad hoc bottom-up emission inventories reflecting lockdown restrictive measures in section 4. We summarize and
confront all the presented estimates in section 5.

2. TROPOMI NO₂ column changes

115 2.1. Dataset and analysis periods

We use the operational Copernicus Sentinel 5 Precursor (S5P) TROPOMI NO₂ level 2 product, for which data have been
available since 28 June 2018. These observations are tropospheric columns (from the surface to the top of the troposphere)
with a pixel resolution of 5.5km by 3.5km since 6 August 2019 and 7km by 3.5km before. The instrument can have up to daily
revisit upon clear sky condition and in this study, we are making use of a quality flag provided with the retrieval, the so called
120 “qa” flag, and only selecting good quality data, i.e. qa > 0.75. This removes cloud-covered scenes, errors and problematic
retrievals (Eskes et al., 2019). We have binned the data on a regular 0.1°x0.1° grid in order to perform statistical analyses and
to facilitate the processing of timeseries for locations of interest, i.e. large European cities in this study (see section 2.2) as well
as the comparison with other datasets such as the 0.1°x 0.1° CAMS regional air quality models (Marecal et al., 2015) and the
9km European Centre for Medium range Weather Forecasts (ECMWF) weather forecasts.

125 In this study we consider February, March and April 2020 and 2019 to assess the changes seen in TROPOMI NO₂ columns
due to COVID-19 restrictions over Europe. Even though the lockdown conditions and dates vary between countries, after 15
March can be considered as a European lockdown as in the middle of the approximate 2-week transition period (e.g. 9 March
2020 in Italy and 23 March 2020 in the UK). We choose to limit our comparisons to the period up to the end of April as a large
portion of countries eased up their lockdown restrictions from the beginning of May onwards. To have an equivalent pre-
130 lockdown period we then include 1 February until 15 March. Table 1 summarizes the periods considered in this study.



Pre-lockdown	Lockdown
From 1 February until March 15	From March 16 until April 30

Table 1. Definition of the 2020 pre-lockdown and lockdown period over Europe considered in this study. Same dates are used for 2019 to perform the comparisons.

135

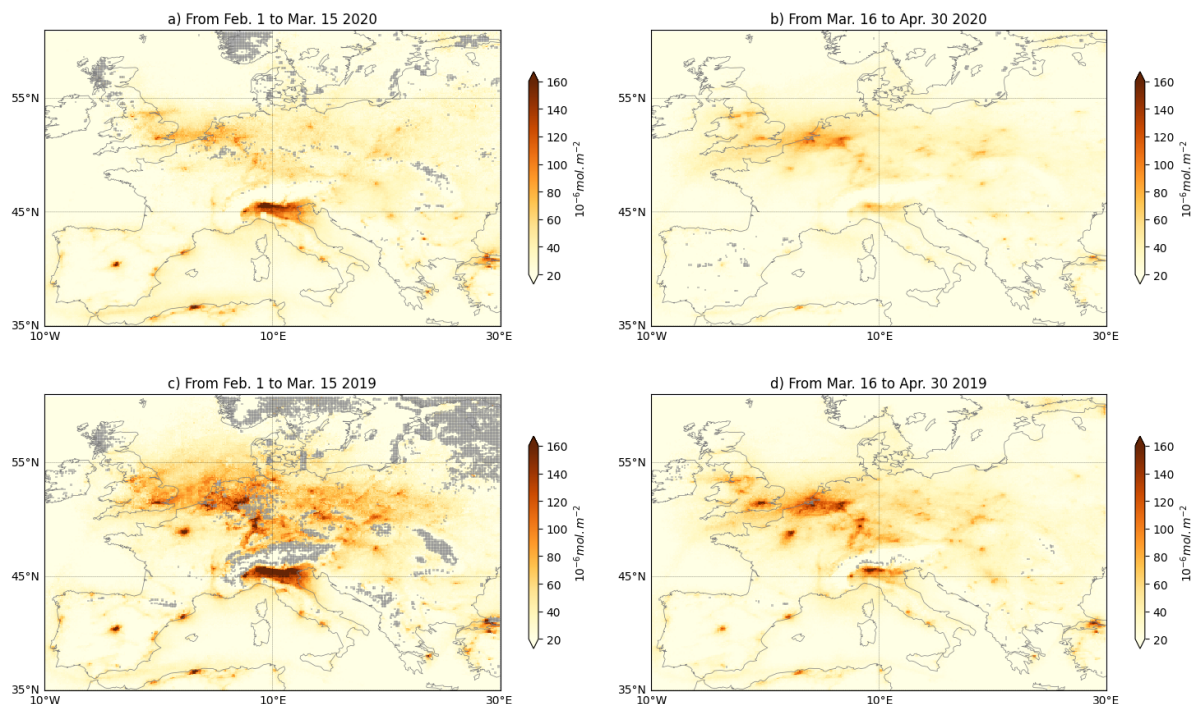
In Figure 1 the $0.1^\circ \times 0.1^\circ$ binned averages are displayed for the pre-lockdown and lockdown period in 2020 and their equivalents in 2019. The comparison of pre-lockdown and lockdown averages for 2020 only shows a decrease in Southern Europe but no clear reduction over more Northern latitudes (i.e. United-Kingdom (UK), The Netherlands and Germany). In the corresponding 2019 pre-lockdown period much larger NO_2 columns than in 2020 are found. During this period of the year, the meteorological conditions over Northern Europe in 2019 and 2020 were significantly different. A number of extratropical cyclones (Ciara, Denis, Karine and Myriam) combined with a strong positive anomaly in temperature occurred over Europe, especially Western and Northern Europe, in February and early March 2020, while no such anomalies in wind and temperature were observed in 2019. Figure 2 shows the distribution of wind speed and planetary boundary layer (PBL) height in both 2019 and 2020 for the pre-lockdown and lockdown periods at the S5P overpass times. The two parameters show very different distributions before 15 March, with much lower values in 2019, i.e. less circulation and vertical dilution of NO_2 leading to increased NO_2 tropospheric columns. During the post-15 March period the distributions are more similar but still show some differences. This illustrates the need for accounting for the meteorological effect when assessing the changes of NO_2 tropospheric columns associated with the lockdown.

140

145

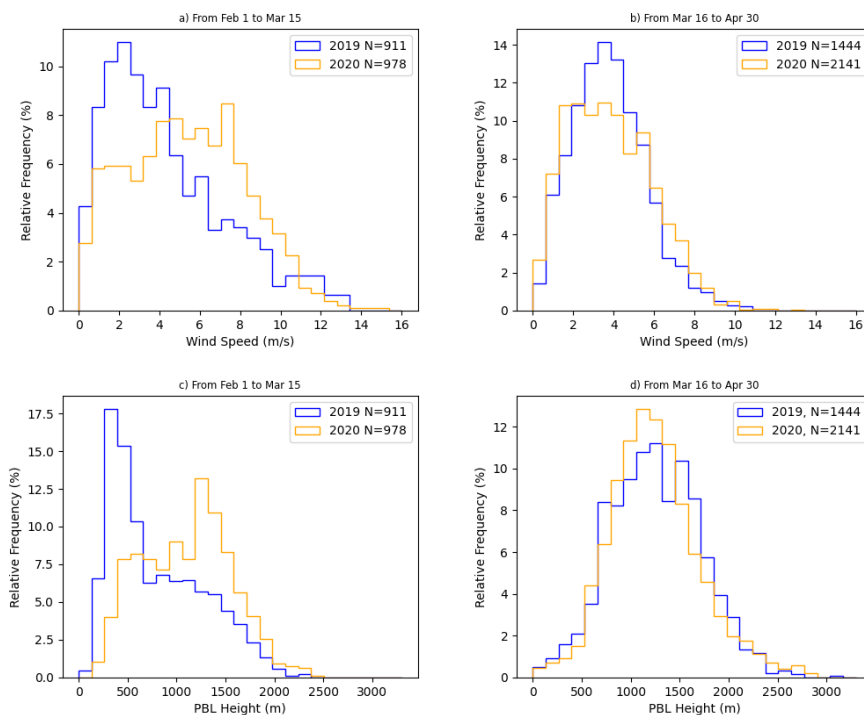


TROPOMI NO₂ time averages



150

Figure 1. Average maps of the TROPOMI NO₂ tropospheric columns (mol.m⁻²) for European pre-lockdown and lockdown periods in 2020 (a, b respectively) and corresponding periods in 2019 (c, d). Grey areas indicate where the number of revisits is strictly below 5.



155

Figure 2. Probability density functions of wind speed ($\text{m}\cdot\text{s}^{-1}$, top) and planetary boundary layer (PBL) height (m, bottom), for European periods before (a,b) and after 15 March (c,d), comparing 2020 to 2019. Distribution are computed for urban areas above 0.5 Million inhabitants between $10^{\circ}\text{W}, 20^{\circ}\text{E}, 45^{\circ}\text{N}$ and 60°N at the S5P overpasses times. N is the sample size for each distribution that can be multiplied by the relative frequency (in %) to obtain the absolute frequency.

160

2.2. Non weather normalized TROPOMI NO_2 column changes estimates

Changes of NO_2 tropospheric columns associated with the lockdown measures can be estimated by comparing NO_2 levels observed during the lockdown period in 2020 with a given baseline. In this section, we compare the results obtained with three different baselines : (1) the NO_2 levels observed during the pre-lockdown period in 2020 (hereafter referred to as the “before-
165 during” approach), (2) the NO_2 levels observed during the same period of the year in 2019 (hereafter referred to as the “year-to-year” approach), and (3) an machine learning-based estimate of the business-as-usual NO_2 levels that would have been observed during the lockdown period in 2020 in the absence of lockdown measures. We focus our study on largest European urban areas exceeding 0.5 million inhabitants, making a total of 100 locations. Assessing the changes of NO_2 tropospheric columns from satellite observations is more challenging over rural areas as the NO_2 levels are much lower than over urban
170 areas. Signal to noise ratio is significantly low in rural areas thus estimates are very sensitive to small changes in the tropospheric columns. We use the TROPOMI NO_2 re-gridded $0.1^{\circ} \times 0.1^{\circ}$ averages filtered according to relevant quality flags



(see section 2.1) and choose the pixels closest to the European city centres and that have more than 5 data points per period defined in Table 1. We first show the reduction estimates over Europe as calculated by examples of non-weather-normalized estimates. The “before-during” estimate corresponds to the difference between pre-lockdown and the lockdown periods. Figure 3 shows changes calculated in that way for 2020 (Fig. 3b) and equivalent in 2019 (Fig 3a) for comparisons. This method shows drastic NO₂ reductions of more than 75% in 2020 for most of large urban areas of Southern Europe. Reductions are not obvious over some of Northern Europe and show strong variations from one city to another. For example, over the UK and Germany some urban areas show increases well above 30% while other urban areas show reductions even though the same lockdown measures were applied nationwide. Applying the same method to data from 2019 shows strong decreases of NO₂ levels in many major European urban areas between the corresponding pre-lockdown and lockdown periods. This illustrates that such “before-during” type of satellite comparisons is misleading and unfit for assessing the effects of COVID-19 lockdown because it is very sensitive to seasonal variations of weather regimes and emissions.

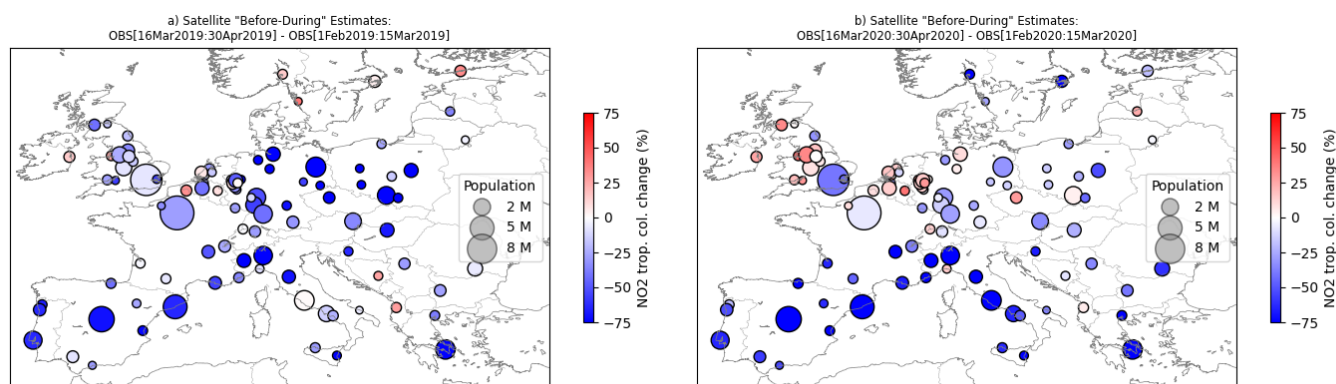
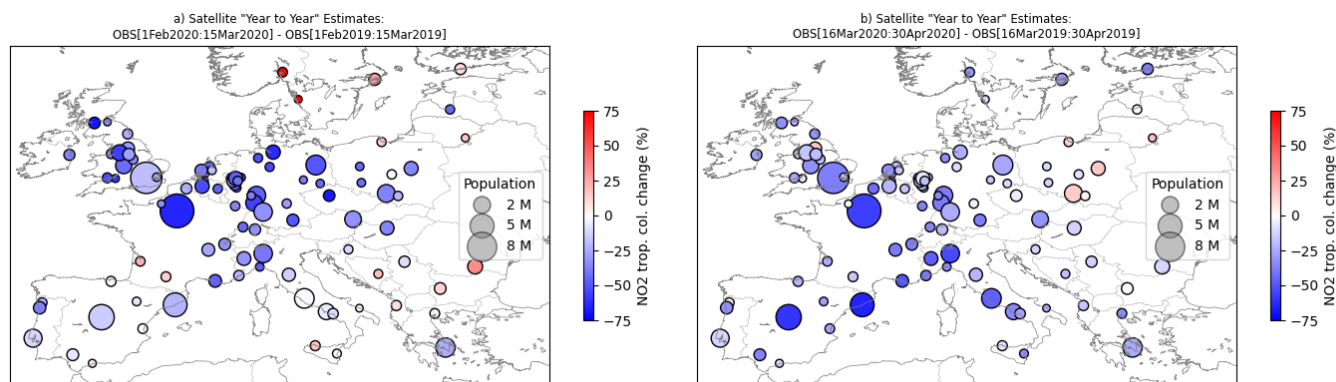


Figure 3. TROPOMI-based estimates of tropospheric NO₂ column change (%) for urban areas above 0.5 million inhabitants computed using pre-lockdown period (from 1 Feb. to 15 Mar.) and lockdown period (from 16 Mar. to 30 Apr.) comparison for 2019 and 2020 (a and b respectively). The diameter of the circles is proportional to the population count in each urban area.

The “year-to-year” approach has been widely used in scientific publications and web press releases is based on comparing 2020 to 2019 data over the period of interest. Figure 4 shows such “year-to-year” estimates for the pre-lockdown (Fig 4a) and lockdown (Fig 4b) periods. During the lockdown an overall reduction is seen all over Europe with more moderate reductions over Southern Europe as compared to the “before-during” estimates (see Figure 3). Northern Europe changes do not show strong city dependent variations and an overall decrease that is not as strong as in Southern Europe. However, looking at the pre-lockdown estimates, Northern Europe shows drastic negative changes, that are actually larger than during the lockdown period, where such deviations from the BAU levels should not be expected. The “year to year” method is strongly dependent on the interannual NO₂ variability even in the BAU situation, where meteorology plays a crucial role. Therefore, this method



can lead to large errors when assessing differences in NO₂ levels and more generally the pollution level reductions due to the COVID-19 lockdown.



200

Figure 4. Satellite observation estimation of tropospheric NO₂ column change (%) for urban areas with at least 0.5 million inhabitants computed using 2019 and 2020 (“year to year”) comparison for the pre-lockdown and lockdown periods (a and b respectively). The diameter of the circles is proportional to the population count in each urban area.

2.3. Weather normalized TROPOMI NO₂ column changes estimates

205

The weather-normalization method accounts for weather variability to estimate the net changes of NO₂ induced by the lockdown in urban areas. We have simulated NO₂ tropospheric columns as TROPOMI would have measured in BAU conditions for 2020, i.e. in the absence of lockdown restrictions. Using meteorological and air pollution predictors to build a simplified model for satellite tropospheric observation simulations or predictions for atmospheric composition have been used in previous studies (e.g. Worden et al., 2013, Barré et al., 2015). In this study, we use a novel approach for satellite observation simulation based on the Gradient Boosting Machine (GBM, Friedman, 2001) regressor technique. GBM is a popular decision tree-based ensemble method belonging to the boosting family. We use weather and air quality variables as predictors from the ECMWF and CAMS operational forecasts at 9km and 0.1° resolutions respectively: 10m wind speed and direction, planetary boundary layer height, 2m temperature, surface relative humidity, geopotential at 500hPa, NO₂ concentrations from the CAMS regional ensemble forecasts (no assimilation) but also latitude, longitude, population, Julian date (number of days since January 1st) and weekday (to reflect expected weekend/weekday effects). Quite similar machine learning (ML)-based approaches have already been successfully applied to in-situ surface AQ observations (e.g. Grange et al., 2018, 2019, Petetin et al., 2020). We use data from 1 January 2019 to 31 May 2019 as a training set and apply the model on 2020 to generate BAU predictions. For validation purposes we have randomly split the data in a 90% and 10% share for training and test, respectively. We then train the model on using the training set only and leaving the test set for final evaluation. Hyper parameter tuning (see annex for

220



225 details) was performed using a grid search method with 5-fold cross-validation and using the ranges indicated by Petetin et al. (2020) that set up a similar method using surface stations. Contrary to Petetin et al. (2020) that trained one ML model per surface air quality monitoring station, only one single ML model is trained here for all cities, due to the small dataset available (about 10,000 data points, see Table 2). After the hyperparameter tuning and evaluation of the model, the observation BAU predictions have been generated using 100% of the January-May 2019 dataset in order to use the maximum amount of data points possible.

	MB [10 ⁻⁶ mol.m ⁻²]	nMB [%]	RMSE [10 ⁻⁶ mol.m ⁻²]	nRMSE [%]	PCC	N
S5P training set	0.00	+0.02	1.4	45.68	0.87	9,634
S5P test set	-0.04	-1.30	1.68	56.38	0.79	1,071

230 **Table 2. Performance of the machine learning predictions of NO₂ tropospheric columns over all European urban areas included in the dataset. The training set and test set includes January-May 2019 and randomly sampled (90% and 10%) over that period.**

235 Detailed scores of the performance of the gradient boosting regressor with respect to the real observations such as mean bias (MB), normalized mean bias (nMB), root-mean-square error (RMSE), normalized root-mean-square error (nRMSE) and the Pearson Correlation Coefficient (PCC) can be found in Table 2. The statistics on both training set and test set show similar results such as low bias, good correlation but significant RMSE. Results indicate that there is no sign of overfitting in the predictions. Since TROPOMI data are available only from mid-2018, the training set is relatively small. For this reason, the predictions are featuring significant RMSE values and will have a large random error. Such RMSE values stay however in the range of surface site air quality machine learning predictions as shown in Section 3 and Table 3. The low mean bias and high correlation values indicate that the main BAU NO₂ tropospheric column variability is represented without large systematic errors. Subtracting the BAU NO₂ simulated columns with the actual observed NO₂ columns during the lockdown period (from 240 16 March 2020 to 30 April 2020) gives us an estimate of the reductions on the NO₂ background levels on the major European urban areas.

245 Figure 5 shows the ML-based BAU equivalent estimates for the pre-lockdown and lockdown periods. The estimates are based on the median value of the real observation minus simulated BAU observation distributions. We choose to display the median and not the mean as the ML estimates are generating strong outliers due to the small training set used. The pre-lockdowns ML estimates do not show as strong overall reductions as in the “year-to-year” (Fig. 4) or “before-during” (Fig. 3) estimates. A summary of the results is provided in Table 3 displaying the average and the standard deviation of NO₂ changes across all



European urban areas considered. The “before-during” and the “year-to-year” approaches also show stronger reduction estimates on average during 2019 and the pre-lockdown period, respectively. Such methods also display a stronger standard deviation across cities than the weather-normalization methods, which suggests substantial biases in the former due to the omission of meteorological variability.

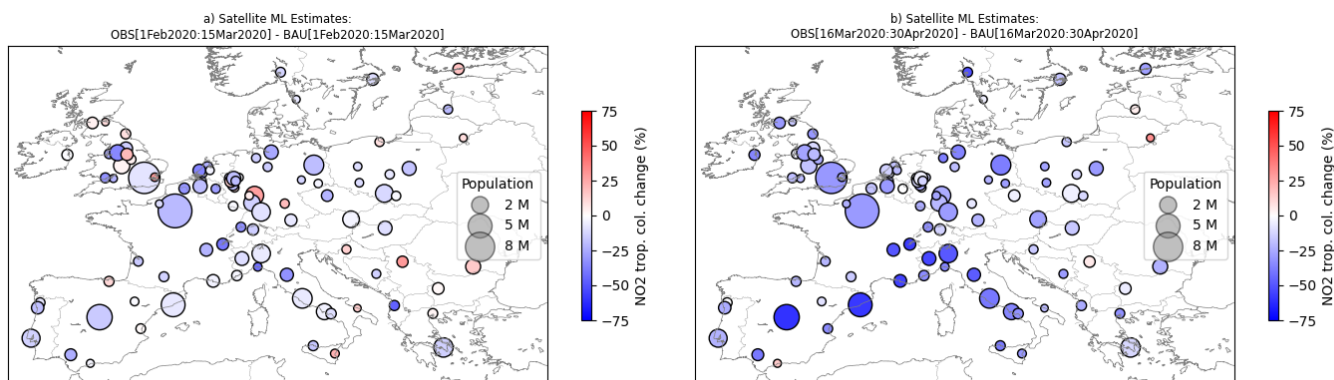


Figure 5. TROPOMI-based estimation of tropospheric NO₂ column change (%) for urban areas with at least 0.5 million inhabitants computed based on the weather-normalization method for the pre-lockdown and lockdown periods (a and b respectively). The diameter of the circles is proportional to the population count in each urban area.

	Average (%)	Standard Deviation (%)
“Before-during” [2019]	-34.45	36.18
“Before-during” [2020]	-30.20	55.55
“Year-to-year” [01/02 to 15/03]	-24.23	28.42
“Year-to-year” [16/03 to 30/04]	-21.78	16.36
Machine Learning [01/02 to 15/03]	-8.27	15.85
Machine Learning [16/03 to 30/04]	-22.72	15.51

Table 3. Scores over all European urban areas included in the dataset for the different TROPOMI NO₂ tropospheric columns change estimations. Average and standard deviation are calculated for all urban area resulting estimates, i.e. the standard deviation is a metric of the inter urban area spread.

The weather-normalization method is not devoid of uncertainties. While a value close to zero would be expected during the pre-lockdown period, the method estimates a slight overall reduction of around -8%, partly due to the shortage of training data. It does however perform much better than the year-to-year and before-during methods that estimate a -24% and -30% reduction, respectively, during the pre-lockdown period. In the case of the lockdown period the weather parameter



distributions are much more similar between 2019 and 2020 (Figure 2) and on average across Europe the “year-to-year” and weather-normalized estimates show results in the same range.

3. Surface station estimates

We estimated the impact of the COVID-19 lockdown on surface NO₂ pollution in European areas using the methodology introduced by Petetin et al. (2020), applied to up to date (i.e. unvalidated real-time) hourly NO₂ data from the European Environmental Agency (EEA) AQ e-Reporting (EEA, 2020). We first selected the urban/suburban background stations located within 0.1° from the city centres and applied the quality assurance and data availability screening described in Petetin et al. (2020), using the GHOST metadata (Globally Harmonised Observational Surface Treatment, Bowdalo et al., 2020, in preparation). A total of 164 stations in 77 urban areas were selected. At each station (independently), we estimated the business-as-usual NO₂ mixing ratios that would have been observed during the lockdown period under an unchanged emission forcing. This was done using GBM models fed by meteorological inputs (2-m temperature, minimum and maximum 2-m temperature, surface wind speed, normalized 10-m zonal and meridian wind speed components, surface pressure, total cloud cover, surface net solar radiation, surface solar radiation downwards, downward UV radiation at the surface and boundary layer height) taken from the 31km horizontal resolution ERA5 reanalysis dataset (Hersbach et al., 2020) in addition to other time features (date index, Julian date, weekday, hour of the day). Using the ERA5 reanalysis data set has a consistent model version over time but a lower resolution (31km) in comparison to the ECMWF high resolution 9km operational forecasts used in the TROPOMI estimates. All GBM models were trained and tuned during the past 3 years (2017-2019) and tested in 2020 before the lockdown. Using the last three years is long enough to capture weather variability at each site, but not too long with regards to long-term reduction of NO₂ happening as a result of policy measures across Europe. Contrary to Petetin et al. (2020) that predicted BAU NO₂ at the daily scale, the ML models developed here are predicting NO₂ at the hourly scale (in order to get results collocated in time with TROPOMI overpasses, see below). We then deduced the weather-normalized NO₂ changes due to the lockdown by comparing observed and ML-based BAU NO₂ mixing ratios. Table 4 shows the overall performance of the GBM models on the training and test sets. Statistical results are similar to the TROPOMI NO₂ GBM model. Biases are low and correlation is high and there is a significant RMSE. Statistical scores in the training set and the test set suggest that there is no sign of overfitting in the predictions and show reasonable performance. Note that the RMSE and PCC are deteriorated compared to the statistics obtained over Spain in Petetin et al. (2020), mainly due to the fact that we are here working at the hourly scale. This is demonstrated by the similar results as those of Petetin et al. (2020) that are obtained over this set of European cities when predicting NO₂ at the daily scale (for the test dataset: nRMSE=28%, PCC=0.88, N=11,082).

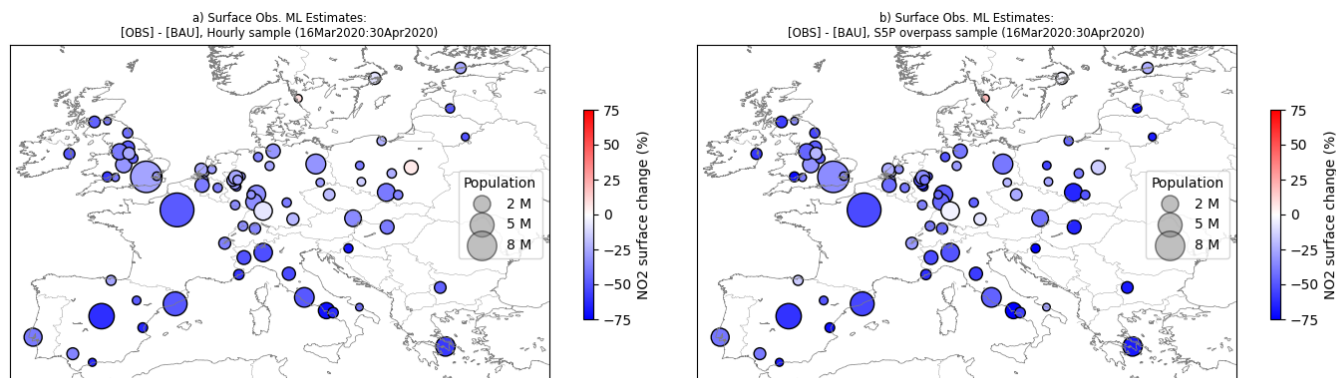
295



	MB [ppbv]	nMB [%]	RMSE [ppbv]	nRMSE [%]	PCC	N
Surface stations training set (2017-2019)	0.0	0.0	5.53	40.88	0.84	4,048,696
Surface stations test set (1 Jan 2020 – 15 Mar 2020)	+0.95	+7.02	6.24	45.87	0.80	268,960

Table 4. Performance of the machine learning predictions of NO₂ surface mixing ratios over all European urban areas included in the dataset.

300 To account for the potential error due to the satellite sampling we provide two estimates: either with complete hourly
sampling or filtered according to with S5P satellite overpass time (13:30 local solar time) and qa filtering (clear sky only)
sampling for a stricter comparison with the results discussed in Section 2. Figure 6 displays relative change estimates, showing
the median of the distributions for each European city above 0.5 million inhabitants. Overall the estimates for both samplings
are broadly consistent, with mean NO₂ changes of around -37% and -43% for the hourly sampling and the S5P overpass
305 sampling, respectively (Table 4). Northern Europe (particularly Germany, Poland and the UK) displays larger reduction with
the estimates at satellite overpass time. In general, those NO₂ relative changes based on surface in-situ concentrations are larger
than the ones based on NO₂ tropospheric columns. This is expected as NO₂ surface site measurement do not directly translates
to the TROPOMI NO₂ tropospheric column, which is the integrated NO₂ content from the surface to about the 200hPa altitude.
Due to the short lifetime of NO₂, only marginal lockdown induced changes of free tropospheric NO₂ contents are expected.
310 Changes are mainly expected near-surface and within the PBL. Also, even if the stations are grouped within a 0.1° range from
the city centres the representativeness of surface observations used might not be similar to a 0.1°x0.1° pixel, depending on the
surface station coverage on each city. This can also exacerbate the difference between surface and tropospheric columns
reduction estimates.



315 **Figure 6. Surface observation estimation of NO₂ changes (%) during the lockdown period using business as usual (BAU) simulated observations for urban areas with at least 0.5 million inhabitants. Left-hand side (a) are the estimates using full hourly datasets and right-hand side (b) are the estimates using S5P overpass time sampled dataset. The diameter of the circles is proportional to the population count in each urban area.**

4. CAMS regional ensemble model estimates

320 Model estimates have been calculated using the CAMS European regional air quality forecasting framework, which is an ensemble of 11 models (CHIMERE, DEHM, EMEP MSC-W, EURAD-IM, GEM-AQ, Lotos-Euros, MATCH, MINNI, MONARCH, MOCAGE, SILAM, Marécal et al. 2015). Using such a multi-model approach is useful to minimize the imperfections in each model's formulation. Two sets of models hindcasts have been conducted using two different emissions scenarios: BAU emissions and reduced COVID-19 lockdown emissions. The emission inventory used for the BAU reference simulation is the same that is used in the daily Regional Air Quality Forecasts of CAMS for Europe, i.e. CAMS-REG-AP (v3.1 for the reference year 2016). It is compiled by TNO under the CAMS emission Service, based on official emissions reported by the countries to the EU (NEC Directive) and UNECE (LRTAP Convention /EMEP) (Kuenen et al., 2014; Granier et al., 2019). The spatial resolution of the emissions is 0.1°x0.05° but later re-gridded at 0.1°x0.1° to match the models' grid. The alternative emission scenario, corresponding to the lockdown period, was derived by combining the original CAMS-REG-AP inventory with a set of country- and sector-resolved reduction factors (Guevara et al., 2020). For the present work, time invariant emission reduction factors were proposed by country and for three activity sectors: manufacturing industry, road transport, and aviation (landing and take-off cycles) that are reduced on average by 15.5%, 54% and 94%, respectively. These sectors were considered to be the most affected by changes in activity during lockdown (Le Quéré et al., 2020). The reduction factors were computed from collections of near-real time activity data, such as Google Community Mobility Reports (Google LLC, 2020) for road transport, airport statistics from Flightradar24 (2020) for aviation and electricity load information from ENTSO-E (2020) for industry. More details about the emission scaling procedure can be found in Colette et al. (2020) where

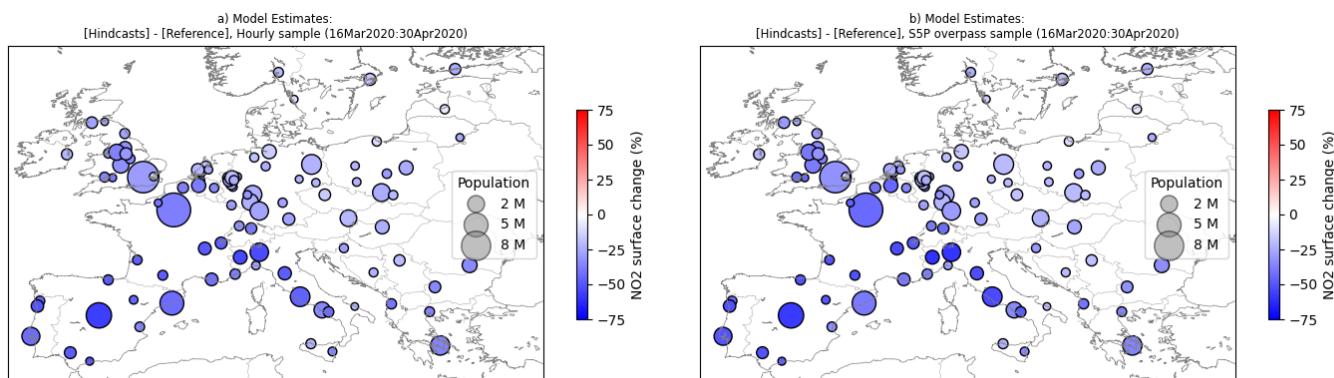
335



the resulting country and activity sector dependent reduction factors are provided for the EU28 countries plus Norway and Switzerland. The largest reductions are observed in those countries where lockdown restrictions were more stringent, such as Italy, Spain and France. All the models operated with the exact same setup as the CAMS regional operational production. The modelling domain covers Europe at $0.1^\circ \times 0.1^\circ$ resolution. The meteorological and chemical boundary conditions are obtained from the Integrated Forecasting System (IFS) of ECMWF, which is the same system that provides part of the dataset for the ML-based estimations (see sections 3.1 and 2.2). The reference simulation was using the BAU anthropogenic emissions as described above and the lockdown scenario was using the same lockdown inventory, modulated by country and activity sectors. From the two sets of 11 model simulations the median at each grid point is calculated from an ensemble simulation (as is routinely done for the operational CAMS predictions, Marecal et al., 2015). Differences between the BAU ensemble and the lockdown scenarios ensemble are then used to calculate model reduction estimates.

Figure 7 displays the relative change estimates for each European city with more than half a million inhabitants, calculating the medians of the full hourly distribution (Fig. 7a) and of the distribution at qa filtered S5P overpasses times and dates only (Fig. 7b). As expected, urban areas in stricter lockdown countries (i.e. Spain, Italy, France) show the largest reductions (e.g. down to 60% in Madrid, see Figure 8) whereas urban areas with softer lockdown measures (i.e. Germany, Poland, Sweden) show milder reductions (e.g. around 16% in Stockholm, see Figure 8). The time sampling difference (hourly versus S5P overpass) does not affect the model estimates much, only few percent differences are seen for most of the European urban areas. In comparison, the surface station estimates show more sensitivity to the time sampling. Table 4 summarises the overall European reduction estimates. On average, the S5P overpass sampling changes the estimates by around -6% for surface station estimates and -1.5% for model estimates. This could suggest a dependence between the time of day and the reduction level (e.g. traffic emissions are peaking daytime hence more reduction should be expected during the day). This topic needs to be further investigated.

360



365 **Figure 7. Surface modelling estimation of NO₂ changes (%) during the lockdown period in urban areas with at least 0.5 million inhabitants. Left-hand side (a) are the estimates using full hourly datasets and right-hand side (b) are the estimates using S5P overpass time sampled dataset. The diameter of the circles is proportional to the population count in each urban area.**

	Average (%)	Standard Deviation (%)
Surface Stations [hourly]	-36.74	15.09
Surface Stations [S5P sampling]	-43.06	18.82
CAMS model ensemble [hourly]	-30.35	10.79
CAMS model ensemble [S5P sampling]	-31.82	11.97
TROPOMI	-22.72	15.51

370 **Table 4. Scores over all European urban areas included in the study for the different NO₂ changes estimates: surface stations, model estimates and TROPOMI. Average and standard deviation are calculated for all urban area resulting estimates, i.e. the standard deviation is a metric of the inter urban area spread.**

5. Summary and Discussions

375 In this paper, we first show the importance of accounting for weather variability in satellite-based estimates of NO₂ changes due to the COVID-19 lockdown. While focusing over Europe and using the TROPOMI instrument, we show that the satellite estimates based on direct comparisons between different time periods without accounting for weather variability can be flawed and should not be used for this kind of assessments. To account for weather variability in satellite estimates, we use a recently developed methodology based on the gradient boosting machine learning technique. This methodology has proven to be efficient with surface sites to estimate lockdown induced changes over Spain (Petetin et al., 2020). We extended those



380 surface estimates over Europe to compare with the satellite estimates. Finally, we included NO₂ changes estimates predicted
by the 11 models CAMS regional ensemble, using emission reduction factors representative of the lockdown period. By
providing and comparing the three different methodologies we provided a comprehensive and complementary assessment of
NO₂ pollution level changes during the COVID-19 European lockdown. Providing such assessment is crucial to accurately
quantify the lockdown pollution changes for air quality policy but also for the impact on the COVID-19 pandemic itself.
Several studies have investigated the correlation between the high level of COVID-19 mortality and atmospheric pollution
385 (e.g. Contincini et al. 2020, Ogen et al. 2020, Achebak et al., 2020). Feedbacks are then to be expected between the effects of
short-term air pollution exposure on COVID-19 mortality and lockdown measures.

In Figure 8 and Table 4 we summarize the results of this study. While Table 4 shows the average reduction with the
inter urban area variability over Europe, Figure 8 shows the difference between the estimates per urban area. For clarity and
relevance, we choose to display only urban areas that are above 1 million inhabitants. The three weather normalized estimates
390 agree on identifying stronger reductions where more severe lockdown measures were implemented. As shown in Section 2
satellite estimates show a relationship between NO₂ tropospheric columns reductions and the extent and generalization of
restrictive measures in each country. A similar relationship is observed for surface sites and model estimates (Sections 3 and
4). The largest NO₂ reduction estimates of around 50% to 60% for both surface and tropospheric column are found for Spanish,
Italian and French urban areas concentrations. In countries that adopted softer lockdown measures urban areas show lower
395 reductions, e.g. Germany, Netherland, Poland or Sweden. Although significant discrepancies exist between the satellite,
surface and model estimates in urban areas such as for example Naples (Italy), Sofia (Bulgaria), Katowice (Poland), the three
methods provide overall a consistent broad picture. This is remarkable to note particularly as satellite data are concerned and
this result contributes to establish their usefulness for urban air quality and not only for atmospheric pollution in general.

Machine learning observation-based estimates display more spread that includes a stronger variability than model
400 estimates. In Figure 8, satellite and surface observation ML estimates show large interquartile ranges, with larger ranges with
satellite for certain urban areas. Such large ranges show that there is a strong spread in the ML based estimates that is not seen
in the model-based estimates. Model estimates are induced by emission country dependent reduction/scaling factors that are
constant over time. In that case variability is induced by the changes in atmospheric conditions but not by changes in the
emissions. The estimates from the ML approach can represent the transition into the lockdown where emission gradually
405 decreased. This is contributing to the increased spread seen in the ML estimates. Scores from ML estimates (see table 2 and
4) also show significant RMSE that can add noise to the time series and then add to the resulting spread of the distributions.
Stronger spread in TROPOMI estimates are likely due to the small training set used. Also, as time goes more TROPOMI data
will be available to strengthen the reliability of the method. Disentangling the noise and the actual variability would need to
be carefully done in further works.

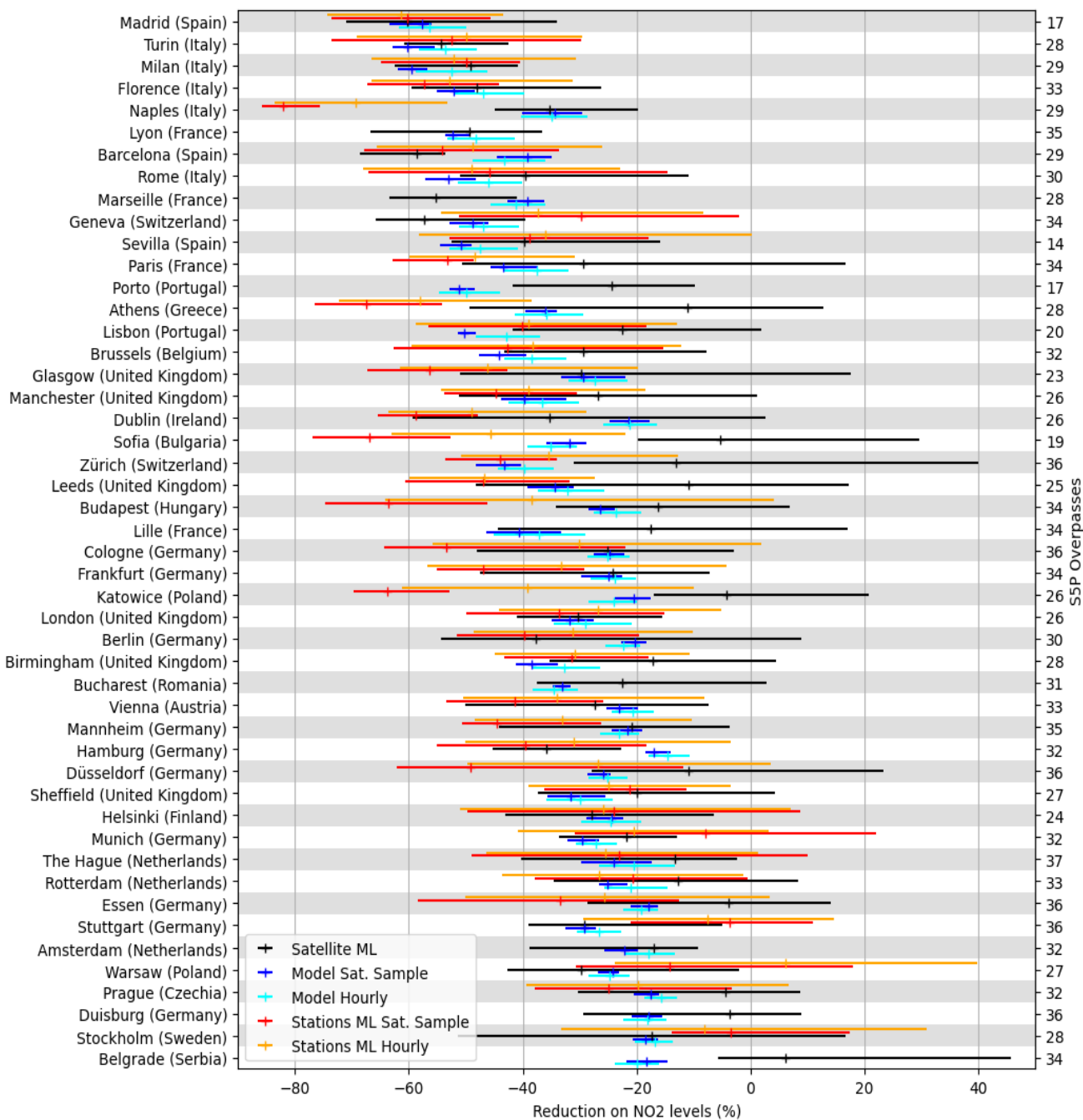
410 In all the different estimates presented above we tried to be consistent in scales using 0.1°x0.1° TROPOMI averaged
pixels that match the CAMS forecasts and background stations within a 0.1° range from the city centre. Some urban areas
considered in this study likely display a background footprint that is finer than 0.1°. The differences seen between surface



station estimates and gridded estimates (models and satellites) point out such possible representativeness issues. Resolution representativeness is a difficult and important topic and deserves further research as it would require higher resolution
415 modelling forecasts and an observation network at a resolution finer than 10km.

Satellite overpass local times and presence of clouds in the measurement pixel can potentially influence the reduction estimates using TROPOMI data. We considered 1.5 months to compute the satellite reduction estimates. Overall the sample size (S5P valid overpasses) in Figure 8 ranges between 14 (Sevilla) and 37 (The Hague). On the same Figure 8, surface sites and model estimates are displayed for hourly and S5P sampled estimates. Smaller or larger samples cannot explain
420 discrepancies between all the different estimates. Results however can be affected when the sample size becomes statistically very small and if shorter time periods (e.g. 1 or 2 weeks) are considered for satellite reduction estimates. Very small samples were not considered in this study. Sampling also shows greater changes in the surface station estimates than in the model estimates. This can suggest that the lockdown-induced reduction estimates could also depend upon the time of the day. Further and more detailed research is needed on this topic.

425 Finally, tropospheric columns NO₂ reduction estimates are mostly smaller than the NO₂ surface estimates (sites and model). The different nature of the vertical sampling (tropospheric columns versus surface concentrations) affects the relative reduction estimates. Some exceptions can be seen in certain Spanish and Italian urban areas where column estimates are close to the surface estimates, but overall column reductions are weaker. Further work will be needed to link quantitatively tropospheric columns and surface levels variations. Including sampling the model estimates using an observation operator
430 commonly used in data assimilation and inverse modelling systems. This important work will be carried out in a further study.



435 **Figure 8. Comparisons of the lockdown induced NO₂ level changes estimates (%) using different means and methodologies for European urban areas above 1 million inhabitants. Horizontal lines represent the interquartile ranges and the ticks are the median values using the full distribution per urban area. For readability, urban areas are ranked using the average between the all median estimates.**



Acknowledgements

440

This project has received funding from the European Union's Horizon 2020 research and innovation programme under the Marie Skłodowska-Curie grant agreement H2020-MSCA-COFUND-2016-754433. Modelling and satellite data were produced by the *Copernicus Atmosphere Monitoring Service*.

445 Annex A. Gradient Boosting Regressor Tuning

We have used TROPOMI data from 2019-01-01 to 2019-05-31 to train our machine learning simulator. We used the gradient boosting regressor function included in the scikit-learn python library. For validation purposes, the data set has been split between a training set (90% of the total dataset) and a test set (10% of the total dataset) using the `train_test_split` function. The hyperparameter tuning is then using the training set to generate the simulators and test set to find the best fit. Similarly, to Petetin et al. (2020) the learning rate was fixed to 0.05 and the number of features (`max_features`) is set to "sqrt". In addition, the tuning of the gradient boosting regressor was done for the following hyperparameters using the grid search method. The following hyperparameters were tuned: the subsample (`subsample` : from 0.3 to 1.0 by 0.1 with a best value of 0.9), the number of trees (`n_estimators`: from 50 to 1000 by 50 with a best value of 400) and the minimum sample in terminal leaves (455 `min_samples_leaf` : from 1 to 30 with a best value of 22). We use the default 5-fold cross-validation. We then test the final results on the test set in order ensure not overfitting.

Links to the python libraries and functions:

Scikit-learn python

460 <https://scikit-learn.org/stable/index.html>

Gradient boosting function

<https://scikit-learn.org/stable/modules/generated/sklearn.ensemble.GradientBoostingRegressor.html>

Grid search hyperparameter tuning

https://scikit-learn.org/stable/modules/generated/sklearn.model_selection.GridSearchCV.html

465 Random dataset splitting

https://scikit-learn.org/stable/modules/generated/sklearn.model_selection.train_test_split.html



470

Annex B. Lockdown induced NO₂ changes estimates for each European urban area considered in this study

Urban Area	Country	TROPOMI Estimates (%)	N Revisits	Model Estimates Hourly (%)	Model Estimates S5P Sampled (%)	Surface Station Estimates Hourly (%)	Surface Station Estimates S5P Sampled (%)
Amsterdam	Netherlands	-17.08	32	-17.93	-22.12		
Antwerp	Belgium	-23.04	36	-21.13	-24.98	-32.79	-30.28
Athens	Greece	-11.13	28	-35.83	-36.06	-58.11	-67.5
Barcelona	Spain	-58.53	29	-43.23	-39.10	-48.81	-54.09
Bari	Italy	-20.13	33	-21.17	-18.29	-44.04	-27.54
Basel	Switzerland	-32.58	37	-31.49	-38.33	-32.95	-38.78
Belgrade	Serbia	6.05	34	-19.86	-18.20		
Berlin	Germany	-37.71	30	-22.27	-20.29	-31.28	-39.73
Bilbao	Spain	-21.29	19	-48.39	-50.45	-26.65	-15.36
Birmingham	UK	-17.24	28	-32.62	-38.41	-30.92	-31.38
Bonn	Germany	-4.55	35	-26.55	-29.04	-38.96	-61.62
Bordeaux	France	-21.59	28	-46.87	-50.39		
Bradford	UK	-24.36	26	-31.31	-33.66		
Braga	Portugal	-1.05	16	-42.93	-42.65		
Bremen	Germany	-37.36	34	-17.99	-19.56	-36.62	-49.47
Brighton	UK	-22.21	31	-20.55	-23.51	-22.75	-27.09
Bristol	UK	-19.47	30	-39.62	-43.63	-38.45	-38.54
Brussels	Belgium	-29.32	32	-38.38	-44.20	-38.16	-42.67
Bucharest	Romania	-22.58	31	-34.50	-33.11		
Budapest	Hungary	-16.18	34	-23.70	-26.36	-38.49	-63.53
Bytom	Poland	-11.97	30	-25.22	-22.21		
Caerdydd	UK	-18.76	31	-35.60	-41.59	-57.81	-72.57
Catania	Italy	-30.34	26	-35.08	-34.75		
Cologne	Germany	-25.04	36	-25.11	-24.74	-30.07	-53.41
Dortmund	Germany	-10.67	36	-23.84	-23.65	-28.63	-48.38
Dresden	Germany	-28.23	32	-21.82	-20.01	-29.26	-21.35
Dublin	Ireland	-35.36	26	-21.27	-21.34	-49.05	-58.8
Duisburg	Germany	-3.73	36	-18.18	-17.91		
Düsseldorf	Germany	-10.86	36	-25.13	-25.92	-26.82	-49.19



Edinburgh	UK	-16.29	23	-27.72	-28.01	-38.95	-34.01
Essen	Germany	-3.92	36	-19.18	-17.85	-25.68	-33.37
Florence	Italy	-48.04	33	-46.88	-52.11	-52.79	-57.22
Frankfurt	Germany	-24.24	34	-23.82	-24.94	-33.22	-46.9
Gdańsk	Poland	-16.67	30	-10.72	-10.09	-23.07	-43.45
Geneva	Switzerland	-57.27	34	-46.85	-48.78	-37.27	-29.81
Genoa	Italy	-35.81	30	-27.19	-26.87		
Glasgow	UK	-29.81	23	-27.33	-29.33	-46.12	-56.41
Gliwice	Poland	-23.30	32	-26.84	-25.04		
Göteborg	Sweden	-4.54	32	-10.18	-13.78	8.84	19.34
Hamburg	Germany	-35.87	32	-14.66	-17.05	-31.01	-39.61
Hannover	Germany	-19.02	33	-23.89	-24.86	-26.09	-29.14
Helsinki	Finland	-27.91	24	-24.63	-24.38	-25.81	-23.97
Katowice	Poland	-4.21	26	-24.03	-20.46	-39.22	-63.85
Kraków	Poland	-11.70	30	-21.07	-20.98	-36.88	-49.36
Leeds	UK	-10.98	25	-32.24	-34.30	-46.82	-47
Leipzig	Germany	-22.63	36	-22.42	-22.65		
Lille	France	-17.46	34	-37.14	-40.67		
Lisbon	Portugal	-22.48	20	-42.92	-50.26	-38.9	-40.18
Liverpool	UK	-3.72	29	-27.72			
Liège	Belgium	-0.44	34	-34.26	-34.95	-37.12	-39.66
Łódź	Poland	-11.58	30	-29.03	-28.65	-23.69	-37.71
London	UK	-30.38	26	-29.02	-31.73	-26.74	-33.58
Lyon	France	-49.43	35	-48.24	-52.33		
Madrid	Spain	-60.18	17	-56.28	-57.69	-61.38	-60.22
Manchester	UK	-26.72	26	-36.51	-39.78	-38.94	-44.68
Mannheim	Germany	-20.89	35	-23.09	-21.60	-33.04	-44.45
Marseille	France	-55.24	28	-41.24	-39.14		
Milan	Italy	-49.13	29	-52.53	-59.50	-52.08	-49.89
Munich	Germany	-21.72	32	-27.08	-29.57	-20.57	-7.93
Málaga	Spain	15.66	6	-50.30	-47.59	-63.08	-66.36
Naples	Italy	-35.28	29	-34.91	-34.39	-69.36	-82
Newcastle	UK	-30.01	22	-27.23	-30.15	-41.78	-53.53
Nice	France	-33.82	24	-38.02	-36.72	-59.47	-60.87
Nottingham	UK	-23.64	23	-34.84	-36.90	-44.84	-46.56
Nuremberg	Germany	-6.95	31	-27.47	-28.10	-38.62	-45.64
Oslo	Norway	-50.93	22	-20.18	-23.63		
Palermo	Italy	-38.72	26	-21.97	-22.73		
Paris	France	-29.37	34	-37.57	-43.43	-48.33	-53.28



Porto	Portugal	-24.41	17	-49.84	-51.19		
Poznań	Poland	-26.43	31	-21.90	-22.05	-38.38	-55.64
Prague	Czechia	-4.47	32	-15.75	-17.60	-19.74	-24.99
Riga	Latvia	5.06	30	-6.84	-7.27	-50.5	-84.04
Rome	Italy	-39.55	30	-46.04	-52.95	-49	-45.74
Rotterdam	Netherlands	-12.73	33	-21.09	-25.21	-26.62	-20.71
Rouen	France	-23.40	35	-39.66	-45.61		
Saarbrücken	Germany	-24.24	38	-27.59	-26.57	-33.47	-37.49
Salerno	Italy	-32.12	26	-42.88	-48.36	-61.57	-56.63
Sarajevo	Bosnia Herz.	-28.87	26	-22.54	-20.07		
Sevilla	Spain	-39.64	14	-47.55	-50.90	-36.1	-38.74
Sheffield	UK	-20.04	27	-29.98	-31.58	-24.87	-21.18
Sofia	Bulgaria	-5.34	19	-35.06	-31.85	-45.72	-66.84
Southend	UK	-26.99	29	-11.26	-11.11	-29.57	-37.41
Stockholm	Sweden	-17.44	28	-16.72	-18.45	-8.11	-3.46
Stuttgart	Germany	-29.26	36	-26.69	-29.23	-7.49	-3.73
The Hague	Netherlands	-13.33	37	-20.57	-24.07	-25.54	-23.09
Thessaloníki	Greece	-32.37	27	-35.97	-35.93		
Tirana	Albania	-24.05	26	-40.06	-40.78		
Toulouse	France	-15.56	24	-47.92	-50.72		
Turin	Italy	-54.29	28	-53.57	-60.29	-49.94	-52.44
Utrecht	Netherlands	-20.40	33	-25.45	-29.52	-28.38	-30.9
Valencia	Spain	-33.54	22	-34.71	-32.98	-63.35	-70.83
Vienna	Austria	-27.27	33	-20.78	-23.04	-34.07	-41.45
Vilnius	Lithuania	32.66	26	-25.18	-23.92	-50.6	-66.15
Warsaw	Poland	-29.68	27	-24.83	-24.20	6.19	-14.19
Wiesbaden	Germany	-26.34	33	-30.11	-31.35	-31.2	-43.57
Wrocław	Poland	-27.53	34	-22.51	-21.09	-14.16	-26.8
Wuppertal	Germany	-12.55	36	-24.56	-24.86	-27.35	-39.35
Zagreb	Croatia	-15.52	32	-28.65	-29.98	-68.09	-81.39
Zaragoza	Spain	-8.44	27	-44.85	-48.94	-47.12	-49.4
Zürich	Switzerland	-13.09	36	-39.70	-43.27	-35.41	-43.96



475 References

- Arya P.S. Air Pollution Meteorology and Dispersion, Oxford University Press, New York (1999)
- Barré, J., D. Edwards, H. Worden, A. Da Silva, W. Lahoz: On the feasibility of monitoring Carbon Monoxide in the lower troposphere from a constellation of Northern Hemisphere geostationary satellites. (Part 1), Atmospheric Environment
480 doi:10.1016/j.atmosenv.2015.04.069, 2015
- Bowdalo, D.: Globally Harmonised Observational Surface Treatment: Database of global surface gas observations, in preparation.
- 485 Bauwens, M. S. Compernelle, T. Stavrakou, J.-F. Müller, J. van Gent, H. Eskes, P. F. Levelt, R. van der A, J. P. Veeffkind, J. Vlietinck, H. Yu, C. Zehner: Impact of coronavirus outbreak on NO₂ pollution assessed using TROPOMI and OMI observations. Geophysical Research Letters, <https://doi.org/10.1029/2020GL087978>, 2020.
- Colette, A., M. Schulz, M. Guevara, B. Raux, A. Mortier, S. Tsyro, F. Meleux, F. Couvidat, C. Geels, M. Gauss, E. Friese,
490 J.W. Kaminski, J. Douros, R. Timmermans, R. Lennart, M. Adani, O. Jorba, R. Kouznetsov, M. Joly, A. Benedictow, H. Fagerli, L. Tarrason, P. Hamer and L. Rouïl, COVID impact on air quality in Europe, A preliminary regional model analysis, CAMS Policy Service Report, 2020, https://policy.atmosphere.copernicus.eu/reports/CAMS71_COVID_20200626_v1.3.pdf
- Collivignarelli, M. C., A. Abba, G. Bertanza, R. Pedrazzani, P. Ricciardi, and M. C. Miino: Lockdown for CoViD-2019 in
495 Milan: What are the effects on air quality? Science of the Total Environment, 732 (139280), <https://doi.org/10.1016/j.scitotenv.2020.139280>, 2020.
- Contincini E., B. Frediani, and D. Caro: Can atmospheric pollution be considered a co-factor in extremely high level of SARS-CoV-2 lethality in Northern Italy? Environmental Pollution, 261, 114465, <https://doi.org/10.1016/j.envpol.2020.114465>,
500 2020.
- EEA: European Union emission inventory report 1990-2018 under the UNECE Convention on Long-range Transboundary Air Pollution (LRTAP), EEA Report No 05/2020, 2020a.



505 EEA: Air Quality e-Reporting Database, European Environment Agency (<http://www.eea.europa.eu/data-and-maps/data/aqereporting-8>) 2020b.

ENTSO-E: Transparency Platform. Available at: <https://transparency.entsoe.eu/> (last accessed, May 2020), 2020.

510 Eskes, H. et al., S5P Mission Performance Centre Nitrogen Dioxide [L2_NO2_] Readme, ESA, 01.03.02. <https://sentinel.esa.int/documents/247904/3541451/Sentinel-5P-Nitrogen-Dioxide-Level-2-Product-Readme-File>

Flightradar24. Airport statistics. Available at: <https://www.flightradar24.com/data/airports> (last accessed, May 2020), 2020.

515 Friedman, J. H.: Greedy function approximation: A gradient boosting machine., *The Annals of Statistics*, 29, 1189–1232, <https://doi.org/10.1214/aos/1013203451>, <http://projecteuclid.org/euclid.aos/1013203451>, 2001.

Goldberg, D. L., Anenberg, S. C., Griffin, D., McLinden, C. A., Lu, Z., & Streets, D. G. (2020). Disentangling the impact of the COVID-19 lockdowns on urban NO₂ from natural variability. *Geophysical Research Letters*, 47, e2020GL089269. <https://doi.org/10.1029/2020GL089269>

Grange, S. K. and Carslaw, D. C.: Using meteorological normalisation to detect interventions in air quality time series, *Science of The Total Environment*, 653, 578–588, <https://doi.org/10.1016/j.scitotenv.2018.10.344>, 2019.

525 Grange, S. K., Carslaw, D. C., Lewis, A. C., Boleti, E., and Hueglin, C.: Random forest meteorological normalisation models for Swiss PM₁₀ trend analysis, *Atmospheric Chemistry and Physics*, 18, 6223–6239, <https://doi.org/10.5194/acp-18-6223-2018>, <https://www.atmos-chem-phys.net/18/6223/2018/>, 2018.

Granier, C., Darras, S., Denier van der Gon, H. A. C., Doubalova, J., Elguindi, N., Galle, B., Gauss, M., Guevara, M., Jalkanen, J.-P., Kuenen, J., Lioussé, C., Quack, B., Simpson, D., and Sindelarova, K.: The Copernicus Atmosphere Monitoring Service global and regional emissions (April 2019 version), Copernicus Atmosphere Monitoring Service (CAMS) report, 2019, <https://doi.org/10.24380/d0bn-kx16>, 2019

535 Google LLC. Google COVID-19 Community Mobility Reports. Available at: <https://www.google.com/covid19/mobility/> (last access: May 2020), 2020



- Guevara, M., Jorba, O., Soret, A., Petetin, H., Bowdalo, D., Serradell, K., Tena, C., Denier van der Gon, H., Kuenen, J., Peuch, V.-H., and Pérez García-Pando, C.: Time-resolved emission reductions for atmospheric chemistry modelling in Europe during the COVID-19 lockdowns, *Atmos. Chem. Phys. Discuss.*, <https://doi.org/10.5194/acp-2020-686>, in review, 2020.
- 540
- Hersbach, H., Bell, B., Berrisford, P., Hirahara, S., Horanyi, A., Muñoz-Sabater, J., Nicolas, J., Peubey, C., Radu, R., Schepers, D., Simmons, A., Soci, C., Abdalla, S., Abellan, X., Balsamo, G., Bechtold, P., Biavati, G., Bidlot, J., Bonavita, M., De Chiara, G., Dahlgren, P., Dee, D., Diamantakis, M., Dragani, R., Flemming, J., Forbes, R., Fuentes, M., Geer, A., Haimberger, L., Healy, S., Hogan, R.J., Holm, E., Janiskova, M., Keeley, S., Laloyaux, P., Lopez, P., Radnoti, G., de Rosnay, P., Rozum, I., Vamborg, F., Villaume, S., Thepaut, J.N. (2020), The ERA5 Global Reanalysis, *Quarterly Journal of the Royal Meteorological Society*, <https://rmets.onlinelibrary.wiley.com/doi/abs/10.1002/qj.3803>
- 545
- Kuenen, J. J. P., Visschedijk, A. J. H., Jozwicka, M., and Denier van der Gon, H. A. C.: TNO-MACC_{II} emission inventory; a multi-year (2003–2009) consistent high-resolution European emission inventory for air quality modelling, *Atmos. Chem. Phys.*, 14, 10963–10976, <https://doi.org/10.5194/acp-14-10963-2014>, 2014
- 550
- Ogen, Y: Assessing nitrogen dioxide (NO₂) levels as a contributing factor to coronavirus (COVID-19) fatality. *Science of the Total Environment*, 72 (138605), <https://doi.org/10.1016/j.scitotenv.2020.138605>, 2020.
- 555
- Iolanda Ialongo, Henrik Virta, Henk Eskes, Jari Hovila, and John Douros, Comparison of TROPOMI/Sentinel-5 Precursor NO₂ observations with ground-based measurements in Helsinki, *Atmos. Meas. Tech.*, 13, 205–218, <https://doi.org/10.5194/amt-13-205-2020>, 2020
- 560
- Le, Tianhao, Yuan Wang, Lang Liu, Jiani Yang, Yuk L. Yung, Guohui Li, John H. Seinfeld, Unexpected air pollution with marked emission reductions during the COVID-19 outbreak in China, *Science* 17 Jun 2020: eabb7431, DOI: 10.1126/science.abb7431
- 565
- Lelieveld, J., Evans, J. S., Fnais, M., Giannadaki, D., & Pozzer, A. (2015). The contribution of outdoor air pollution sources to premature mortality on a global scale. *Nature*, 525(7569), 367– 371. <https://doi.org/10.1038/nature15371>
- Le Quéré, C., R. B. Jackson, M. W. Jones, A. J. P. Smith, S. Abernethy, R. M. Andrew, A. J. De-Gol, D. R. Willis, Y. Shan, J. G. Canadell, P. Friedlingstein, F. Creutzig and G. P. Peters: Temporary reduction in daily global CO₂ emissions during the COVID-19 forced confinement. *Nature Climate Change*, <https://doi.org/10.1038/s41558-020-0797-x>, 2020.



570 Marécal, V., Peuch, V.-H., Andersson, C., Andersson, S., Arteta, J., Beekmann, M., Benedictow, A., Bergström, R., Bessagnet,
B., Cansado, A., Chéroux, F., Colette, A., Coman, A., Curier, R. L., Denier van der Gon, H. A. C., Drouin, A., Elbern, H.,
Emili, E., Engelen, R. J., Eskes, H. J., Foret, G., Friese, E., Gauss, M., Giannaros, C., Guth, J., Joly, M., Jaumouillé, E., Josse,
B., Kadyrov, N., Kaiser, J. W., Krajsek, K., Kuenen, J., Kumar, U., Liora, N., Lopez, E., Malherbe, L., Martinez, I., Melas,
D., Meleux, F., Menut, L., Moinat, P., Morales, T., Parmentier, J., Piacentini, A., Plu, M., Poupkou, A., Queguiner, S.,
575 Robertson, L., Rouïl, L., Schaap, M., Segers, A., Sofiev, M., Tarasson, L., Thomas, M., Timmermans, R., Valdebenito, Á.,
van Velthoven, P., van Versendaal, R., Vira, J., and Ung, A.: A regional air quality forecasting system over Europe: the MACC-
II daily ensemble production, *Geosci. Model Dev.*, 8, 2777–2813, <https://doi.org/10.5194/gmd-8-2777-2015>, 2015.

Manuel A. Zambrano-Monserrate, María Alejandra Ruano, Luis Sanchez-Alcalde, Indirect effects of COVID-19 on the
580 environment, *Science of The Total Environment*, Volume 728, 2020, 138813, ISSN 0048-9697,
<https://doi.org/10.1016/j.scitotenv.2020.138813>.

Muhammad, S., X. Long, and M. Salman: COVID-19 pandemic and environmental pollution: A blessing in disguise? *Science
of the Total Environment*, 728 (138820), <https://doi.org/10.1016/j.scitotenv.2020.138820>, 2020.
585

Myhre G. et al., “Anthropogenic and natural radiative forcing” in *Climate Change 2013: The Physical Science Basis. Contribution of Working Group I to the Fifth Assessment Report of the Intergovernmental Panel on Climate Change*, T. F. Stocker et al., Eds. (Cambridge University Press, Cambridge, United Kingdom, 2013), pp. 659–740.

590 Nakada, L. Y. K. and R. C. Urban: COVID-19 pandemic: Impacts on the air quality during the partial lockdown in Sao Paulo
state, Brazil. *Science of the Total Environment*, 730 (139087), <https://doi.org/10.1016/j.scitotenv.2020.139087>, 2020.

Petetin, H., Bowdalo, D., Soret, A., Guevara, M., Jorba, O., Serradell, K., and Pérez García-Pando, C.: Meteorology-
normalized impact of COVID-19 lockdown upon NO₂ pollution in Spain, *Atmos. Chem. Phys. Discuss.*,
595 <https://doi.org/10.5194/acp-2020-446>, in review, 2020.

Schiermeier. Q: Why pollution is falling in some cities but not others. *Nature*, 580 (7803),
313. <https://doi.org/10.1038/d41586-020-01049-6>, 2020.

600 Seinfeld, John H., and Spyros N. Pandis. 2006. *Atmospheric chemistry and physics: from air pollution to climate change*.
Hoboken, N.J.: J. Wiley.



605 Veefkind, J. P., Aben, I., McMullan, K., Förster, H., de Vries, J., Otter, G., et al. (2012). TROPOMI on the ESA Sentinel-5
Precursor: A GMES mission for global observations of the atmospheric composition for climate, air quality and ozone layer
applications. *Remote Sensing of Environment*, 120, 70–83. <https://doi.org/10.1016/j.rse.2011.09.027>

610 Wang, Y. Y. Yuan, Q. Wang, C. Liu, Q. Zhi, and J. Cao: Changes in air quality related to the control of coronavirus in China:
Implications for traffic and industrial emissions. *Science of the Total Environment*, 731
(139133), <https://doi.org/10.1016/j.scitotenv.2020.139133>, 2020a.

Wang, Q. and M. Su: A preliminary assessment of the impact of COVID-19 on environment - A case study in China. *Science
of the Total Environment*, 728 (138915), <https://doi.org/10.1016/j.scitotenv.2020.138915>, 2020b.

615 Worden, H. M., Edwards, D. P., Deeter, M. N., Fu, D., Kulawik, S. S., Worden, J. R., & Arellano, A. (2013). Averaging kernel
prediction from atmospheric and surface state parameters based on multiple regression for nadir-viewing satellite
measurements of carbon monoxide and ozone. *Atmospheric Measurement Techniques*, 6(7), 1633-
1646. <https://doi.org/10.5194/amt-6-1633-2013>